Available online at www.sciencedirect.com

ScienceDirect

journal homepage: http://www.elsevier.com/locate/rpor

Original research article

Intensity-modulated radiation therapy and volumetric modulated arc therapy versus conventional conformal techniques at high energy: Dose assessment and impact on second primary cancer in the out-of-field region

Beatriz Sánchez-Nieto[a,b,*], *Maria Romero-Expósito*[c], *José Antonio Terrón*[d], *Leticia Irazola*[e], *Marta Paiusco*[f], *Elisabetta Cagni*[f], *Caterina Ghetti*[g], *Silvano Filice*[g], *Francisco Sánchez-Doblado*[d,e]

[a] *Instituto de Física, Pontificia Universidad Católica de Chile, Santiago, Chile*
[b] *Center UC Investigation in Oncology at Pontificia Universidad Católica de Chile, Pontificia Universidad Católica de Chile, Santiago, Chile*
[c] *Departament de Física, Universitat Autònoma de Barcelona, Bellaterra, Spain*
[d] *Servicio de Radiofísica, Hospital Universitario Virgen Macarena, Sevilla, Spain*
[e] *Departamento de Fisiología Médica y Biofísica, Universidad de Sevilla, Sevilla, Spain*
[f] *Veneto Institute of Oncology IOV – IRCCS, Padua, Italy*
[g] *Servizio di Fisica Sanitaria, Azienda Ospedaliera Universitaria di Parma, Italy*

ARTICLE INFO

Article history:
Received 26 August 2017
Received in revised form
19 January 2018
Accepted 12 April 2018
Available online 18 May 2018

Keywords:
Second primary cancer
Peripheral doses in radiotherapy

ABSTRACT

The aim of this work was to estimate peripheral neutron and photon doses associated with the conventional 3D conformal radiotherapy techniques in comparison to modern ones such as Intensity modulated radiation therapy and volumetric modulated arc therapy. Assessment in terms of second cancer incidence ought to peripheral doses was also considered. For that, a dosimetric methodology proposed by the authors has been applied beyond the region where there is no CT information and, thus, treatment planning systems do not calculate and where, nonetheless, about one third of second primary cancers occurs.

* *Corresponding author at*: Instituto de Física, Pontificia Universidad Católica de Chile, Santiago, Chile.
E-mail address: bsanchez@gmail.com (B. Sánchez-Nieto).

https://doi.org/10.1016/j.rpor.2018.04.008

1. Introduction

Intensity modulated radiotherapy (IMRT)[1] and volumetric modulated arc therapy (VMAT)[2] are usually associated, in comparison with three dimensional conformal radiotherapy (3D-CRT), not only to the reduction of volumes irradiated to high dose levels, but also to the significant increase of volume exposed to low doses due to the increase in the number of beam entries and, usually, of monitor units (MUs). These out-of-field doses are related to the secondary malignancies.[3,4] According to Diallo et al.[4] more than 70% of second malignancies would occur outside the irradiated volume (ICRU definition), named as out-of-field or peripheral region from now onwards.

The increased concern about second primary cancer risk has led to a substantial number of works focusing on the evaluation of out-of-field doses. For example, Xu et al.[5] and Gudowska et al.[6] have published interesting reviews about this topic. In photon radiotherapy (RT), out-of-field doses are due to photons scattered inside the body and in the linac head components, as well as those leaking through the linac head. This unwanted photon dose is increased by the neutron contribution during high energy (i.e., $\geq$10 MV) photon RT treatments.[7] However, neutrons have been frequently ignored, in contrast to photon dosimetry, due to the lack of adequate evaluation procedures. In this sense, our group has recently developed a systematic methodology to quantify neutron absorbed doses to organs.[8–11] This lack of established methods for out-of-field dosimetry prevented the estimation of second primary cancer risks associated to specific treatments. And yet, the ability to estimate equivalent organ doses (even retrospectively) is essential for epidemiology studies intended to improve radiocarcinogenesis models.

In the past, 3D-CRT high energy treatments were common for pelvic irradiation since the target is located deep inside the body.[12] The arrival of highly-demanding MUs techniques (e.g., IMRT, VMAT, etc.), presented the dilemma in deciding whether or not to continue using high energy. In fact, based on results showing no clear clinical benefit with the high energy, some works recommended the low-energy photon beams for IMRT.[13] The low energy IMRT plans, in general, can be clinically equivalent to those with high energy in terms of target coverage, homogeneity, and conformity; but with the advantage of no neutron production. However, this is generally achieved at the cost of an increased number of Monitor Units (MUs) and so larger low-dose peripheral volumes. Nonetheless, the new techniques were frequently implemented at low energy, being the latter the current preference.[12] That is, simply because there is not clear quantification of the disadvantages, which allow the proper risk-benefit judgement. A recent review[14] evaluates a significant number of published data, but mainly focused on conventional treatments and encouraging to its extension to modern techniques.

The dosimetric methodology used in this work, is based on two different models developed by our group to estimate the neutron[11] and photon[15] peripheral equivalent dose to cancer-at-risks organs for patients undergoing photon RT. Despite being responsible from a significant fraction of second cancers, this low-dose region is frequently ignored. For example, according to Berrington et al.[16] approximately 80% of the second cancers were observed far from the beams portals after 2D and 3D prostate cancer RT (i.e., excluding rectal and bladder second cancers from the total number of second cancers).

Our models allow the estimation, even retrospectively, of neutron and photon dose to out-of-field organs, beyond the region where commercial treatment planning systems are not intended to calculate accurately.[17] Moreover, the models used take into consideration patient's size without the need of the patient's whole body CT scan (which is not usually available).

The aim of this work was to quantify the impact, in terms of peripheral low-doses, and, subsequently, of the risk of second primary cancers, of using clinically relevant high energy IMRT and VMAT vs. 3D-CRT treatment plans. That is to what extent high energy IMRT-VMAT plans are a sensible alternative to high-energy 3D-CRT in terms of peripheral doses.

2. Methods

2.1. *Radiotherapy plans*

Three tumour sites (prostate, rectum and cervix) were chosen. Treatments were planned on available patient CT sets, so that the Planning Target Volume (PTV) and organs at risk (OAR) could be drawn. Four different scenarios, 3D-CRT and VMAT at 15 MV plans and 3D-CRT and IMRT at 18 MV plans, were generated for each treatment site and then delivered to an anthropomorphic RANDO® phantom (Radiology Support Devices Inc., Long Beach, CA) (Fig. 1). A Varian DHX 2100 linac unit (Varian Medical System, Palo Alto, CA) was used for the 15 MV VMAT and 3D-CRT treatments, whereas a Varian Clinac 2100 C/D (Varian Medical System, Palo Alto, CA) was used for the IMRT and 3D-CRT at 18 MV. A DHX 2100 Linac Unit.

All plans were created so that at least 95% of the prescribed dose (different for each tumour site) was delivered to 100%

Fig. 1 – Experimental set-up for neutron dose measurement during the irradiation of the anthropomorphic RANDO® phantom. The digital detector used during treatment delivery is highlighted. It can be noted that the detector position does not interfere with the routine clinical activity, as it does not need to be close to the patient.

Table 1 – Characteristics of the treatments delivered to the anthropomorphic phantom. All treatments listed here were delivered with coplanar beams.

Tumoursite	Dose to 95% isodose (Gy)	Energy (MV)	Technique	MU	Other
Prostate	70	15	3D-CRT	9338	7 incidences
			VMAT	18247	1 arc
		18	3D-CRT	11585	5 incidences, physicwedge
			IMRT	36526	5 incidences
Rectum	45	15	3D-CRT	6777	3 incidences, virtual wedge
			VMAT	8964	2 arcs
		18	3D-CRT	5171	4 incidences
			IMRT	21717	5 incidences
Cervix	45	15	3D-CRT	6147	4 incidences
			VMAT	14139	2 arcs
		18	3D-CRT	5742	4 incidences
			IMRT	27099	7 incidences

of PTV and that the physical dose-volume constraints on the OAR met acceptable clinical criteria. All prostate plans fulfilled the dose-volume constraints recommended by Gulliford and colleagues.[18] As soon as these goals were achieved, no extra attempt was made in terms of further improving the OAR sparing or decreasing the number of MUs (compatible with tumour prescription). Main characteristics of the treatment plans have been summarized in Table 1. Plans were created using Eclipse™ treatment planning system v. 8.6 and 8.1for the 15 MV and 18 MV treatments, respectively. For IMRT plans, inverse planning was used with no more than 7 field entries. The 15 MV rectum and 18 MV 3D-CRT prostate cases required the use of wedges, which is reflected in the increased number of total MUs. Once the plans were created, they were delivered to one anthropomorphic Alderson RANDO® phantom (Fig. 1).

2.2. *Peripheral dose determination*

Depending on the dose level, either the dose calculation and/or the risk models should deserve different considerations as Harrison nicely discussed.[19] More specifically, up to 3–4 Gy (i.e., ≈5% of current RT prescription doses) seems to be reasonable to adopt the linear no threshold (LNT) model.[20–22] However, the accuracy of commercial treatment planning systems (TPS) might be questioned at such distances from the target volume.[23] Within the volume enclosed by the 5% isodose curve (high to medium dose), TPS should calculate doses accurately but a greater uncertainty for risk estimation models, due to the incomplete understanding of non-linear effects such as cell sterilization and repopulation, might exits. Nevertheless, foundation for secondary risk estimations lies in the reliable knowledge of dose to organs.

As the high to medium dose region is covered by the TPS, this work will focus on using a robust dosimetric methodology to determine photon and neutron doses in the low dose region. The later for the evaluation and comparison of secondary cancer risks associated to IMRT or VMAT vs. 3DCRT at high energies.

The 9 RT plans described in Table 1, were delivered to the anthropomorphic phantom. During the irradiations, a thermal neutron digital detector,[24] allowing the application of the neutron equivalent dose determination (see Section 2.2.1), was used. No photon detector was required as the photon doses are determined by means of an analytic model (see Section 2.2.2)

2.2.1. *Neutron equivalent dose*

The neutron model used[11] approximates the equivalent dose to organs to the average of dose equivalent at a few points that represent the organ of interest for second cancer estimations. In that model, the dose equivalent per unit neutron fluence at a given point was theoretically obtained by folding the following three energy-dependent quantities: the neutron spectrum derived from Monte Carlo (MC) simulation, the fluence-to-kerma conversion coefficient[8] and the radiation weighting factors given in ICRP-103.[21] Finally, the dose equivalent at a point in a tissue was determined by multiplying the resulting quantity by the total neutron fluence measured in-phantom with passive detectors. This dose equivalent, which approximates the equivalent dose in an organ of interest, was correlated with the readings of a neutron digital detector[8–11] located inside the treatment room during phantom irradiation. The above methodology allowed the development of a correlation model which, applied to the digital detector readings during patient irradiation, enables the on-line estimation of neutron equivalent dose to organs.[8–11]

In particular, the neutron equivalent dose to k-organ ($H^{n}_{T,k}$) can be obtained from the following equation:

$$[H]_T^{k,j}(\mu Sv) = R \cdot [E(HW)]_{k,j} \quad (1)$$

where R can be either estimated by means of the facility characterization approach[8,10] or directly measured[11] (the latter is the case of this study). $[E(HW)]_{k,j}$ are the corresponding equations for every k-organ for a j-treatment location and regarding patient size.[11] The uncertainty in the neutron equivalent dose to organs, estimated using this methodology, was at least 30% (1 SD), which included the uncertainties associated to: the digital detector readings and the bunker size factor. Remarkably, this uncertainty is dominated by the last factor due to the dispersion of the values measured at 6 different institutions.[8] This neutron dosimetric methodology has been successfully tested by means of and independent set of neutron detectors.[25,26]

Due to difficulties raised on photon rejection when estimating neutron doses, this model was originally established for points at distances larger than 10 cm from the 50% isodose.

However, as neutron fluence does not drastically depend on distance to the treatment field, it has been assumed reasonable to extend the calculation to all points outside the 5% isodose. This assumption is not critical anyway as neutron doses are not the main contribution to the peripheral dose, especially at this close regions of high photon contribution.

In the present study, R in Eq. (1) was provided by a digital detector[24] placed inside the bunker during the actual delivery of each plan (Fig. 1) whereas the $[E(HW)]_{k,j}$ values were calculated using height and weight of the anthropomorphic RANDO® phantom.

2.2.2. *Photon equivalent dose*

The analytical photon model evaluates the contribution to the peripheral dose of scatter and leakage photons.[15] Firstly, a dose at points basic model was proposed and parameterized by fitting it to absorbed doses measured with TLD-700 in a humanoid phantom during a "reference" irradiation with open beams. The basic model was then modified to account for any field shape, size and degree of modulation. The equivalent dose to organs model was proposed as the integration of absorbed dose at points along the organ length (estimated by rescaling the individual anatomical dimensions onto a mathematical phantom with internal organs). Note that this approximation is valid as the model operates in the low-dose region where tissue response is assumed to be linear.

Photon dose at points was calculated following the model described in Sánchez-Nieto et al.[15] The model allows, for isocentric treatments, calculating the absorbed dose (termed, peripheral photon dose – *PPD*) at any point placed at a distance x from the isocenter of the treatment and at the same depth z using the following equation:

$$PPD(x, z, f, \in) = A + \frac{B}{x^2} \in F(f)e^{-r_{eff}} \quad (2)$$

where A represents the component due to leakage, assumed as constant, and the second term accounts for the radiation scattered in the linac head. The latter was modelled as the result of a virtual source of radiation emitting isotropically from the linac head which falls off as the inverse-square law ($\sim B/x^2$) and the exponential attenuation in air and tissue ($\sim e^{-r_{eff}}$). Additionally, the effect of the efficiency in the use of MUs and the field size is considered through factors $\in$ and $F(f)$, respectively. We refer the reader to the work describing the model[15] for a detailed explanation of parameters and their appropriate values. The largest relative uncertainty of the model was ±25%.

Finally, photon equivalent dose to organ $k(H^{\gamma}_{T,k})$ is calculated as the weighted sum of *PPD* at points along the cranio-caudal axis of the organ. A validation of the *PPD* at points and dose-to-organ models has been carried out with TLD-100 placed inside an Alderson phantom.[27] TLD-100 measurements and calculations showed excellent agreement up to points lying on the 5% isodose.

2.3. *Second cancer risk models*

Despite the main goal of our work was the calculation of peripheral doses, we considered that it would be of interest to perform a first assessment of the associated second primary cancer risks. For that, recommendations by the International Commission on Radiological Protection (ICRP) and the biological effects of ionizing radiations (BEIR) were followed. There are several sources for the uncertainties in radiation risk estimates. Apart from statistical uncertainties, there are other factors that can be encompassed as the transfer of risk estimates between different populations. For example, applying the risks estimates from the life span study (LSS) cohort of atomic survivors to low-dose or chronic exposures (using the dose and dose-rate effectiveness factor, the so called DDREF). There are also differences across populations with respect to prevalence of modifiers of radiation-related risks (such as smoking habits for lung cancer assessment) or of baselines cancer rates, or the relative biological effectiveness, relative to the high-energy photons of the LSS cohort to the different beam qualities during medical exposures. ICRP 103 and BEIR VII extensively elaborate about that.

In RT, prescription doses prescribed are usually below 90 Gy, and therefore the maximum dose at points lying outside the 5% isodose would be ≤4.5 Gy. According to Schneider et al.,[23] this dose is about the upper limit for the use of a linear non-threshold (LNT) response to dose of the cancer incidence rate. Moreover, in Shuryak et al.[28,29] the best fit models prediction for separate organs corroborate Schneider's statement for even larger doses (e.g., 35 Gy approximately for lung). Only colon, according to Shuryak, would show a nonlinear behaviour to very low doses (up to 2 Gy). Moreover, ICRP 99[20] states that LNT theory remains a prudent basis for radiation protection at low doses and low dose rates.

In this work, total equivalent dose to organs in the low dose region were largely below 3 Sv. Therefore, whatever is the case of acute or protracted irradiation, the same LNT model is valid.

Organ-specific second cancer incidence risks were then estimated from the total equivalent dose to the organ ($H_{T,k}$), computed as the sum of the neutron and photon equivalent doses, as follows:

$$R_k = \lambda_k \cdot H_{T,k} = \lambda_k \cdot (H^{n}_{T,k} + H^{\gamma}_{T,k}) \quad (3)$$

being λ_k the appropriate risk coefficient.

ICRP uses nominal risk (after an average latency period of 10 years) whereas BEIR uses lifetime attributable risk (LAR) after a latency period of 5 years for solid cancers and 2 years for leukaemia. Although both models are primarily based on the LSS study, they present some differences. ICRP-103 coefficients were derived from averages across Asian and Euro-American populations, and BEIR-VII coefficients, from the US population. They also chose different DDREF values for cancer risk estimation (values of 2 and 1.5 for ICRP-103 and 1.5 for BEIR VII, respectively). Additionally, ICRP-103 risk estimates are sex- and age-at-exposure-averaged, whereas BEIR-VII estimates are also specific for these parameters. For the BEIR-VII *SPCR* estimations in this work, the age-averaged coefficients (Table 12-5A in BEIR report[22]) were used in order to allow a comparison with ICRP values (Table A.4.1).

In this work, the second primary cancer risk (*SPCR* hereafter) was estimated as the sum of the site-specific risks for all of the organs considered by ICRP and BEIR. The set of common organs for both protocols is: thyroid, lung, breast (for females),

stomach, liver, colon, urinary bladder, and red marrow. ICRP also considers oesophagus, bone, skin and a remainder group including prostate for males and uterus for females. Conversely, those organs are considered independently in BEIR report. Additionally, as no specification of remainder is done in BEIR (it is just referred as "other solid"), calculations following that recommendation were carried out as in ICRP but including oesophagus and excluding prostate/uterus. Despite the fact that $DDREF_{ICRP} > DDREF_{BEIR}$, not all the risk coefficients for the organs in common to both protocols were smaller in the ICRP-103 than in BEIR-VII. This might be due to the impact of differences among the populations and latency times used to derive the coefficients by the two commissions.

As previously mentioned, we focused our attention in organs completely outside the 5% isodose volume or the portion of the organ not enclosed by the 5% isodose curve. Therefore, rectal second cancers (for prostate or gynaecological irradiations) were not considered. The equivalent dose to bladder and second cancer determinations corresponded to the portion of the bladder in the low dose region.

3. Results and discussion

Tables 2 and 3 show photon and neutron equivalent doses to the selected organs for the different tumour locations and techniques. Prostate does not appear in the tables because either it was totally enclosed by the 5% isodose curve or the pathology was specific to females (i.e., cervix). Neutron peripheral dose values obtained are compatible with the linear models by Expósito et al.[9]. For example, in the current exercise, average neutron equivalent dose in liver for the irradiations carried out at the Varian Clinac 2100 at 18 MV with 10.000 MU would be 43.3 mSv, which coincides with the value predicted by the linear regression showed in Expósito et al.[9]

Photon peripheral dose to organ (H_T^γ) ranged from 16 mSv to the thyroid for the 15 MV 3D-CRT rectum treatment to 121 mSv to bladder in the IMRT 18 MV prostate treatment. This result is consistent with the fact that H_T^γ is mainly dependent on the distance to the border of the field and precisely, for each treatment, the highest value was obtained for the closest organ to treatment field (urinary bladder), while the lowest for the furthest organ (thyroid). Neutron peripheral dose (H_T^n) ranges from 760 mSv to skin for the 18 MV IMRT prostate treatment to 4.65 mSv to the colon for the 15 MV 3D-CRT rectum treatment. For each treatment, neutron equivalent doses are dominated by the depth of the organ or tissue, leading then to the highest H_T^n to skin.

Apart from the impact of the organ location on the equivalent dose to organ (H_T) and linac unit, the beam-on-time and energy are the other relevant parameters to look at. For example, the larger the MUs, the larger the photon and neutron equivalent doses, provided the other factors are kept constant. Finally, beam energy affects differently to photon and neutron equivalent doses. In the case of photons, the energy dependence was considered negligible and therefore not included in the model (Eq. (2)) whereas neutron dose follows the photonuclear cross section dependence with energy. Therefore, there will be cases where the number of MUs and energy,

Table 2 – Photon equivalent dose to organs obtained for the different tumour sites and techniques.

Location	Energy	Technique	H_T (mSv)																
			Thyroid	Lung	Breast	Stomach	Oesophagus	Liver	Colon	Urinary Bladder	Ovary	Uterus	Prostate	Red Marrow	Bone	Skin	Rem. ICRP male	Rem. ICRP female	Rem. BEIR
Prostate	18	3D-CRT	35	35	–	35	35	35	41	46	–	–	–	39	36	36	32	–	35
		IMRT	110	110	–	110	110	110	116	121	–	–	–	114	110	111	99	–	110
	15	3D-CRT	28	28	–	28	28	28	34	39	–	–	–	32	29	29	26	–	28
		VMAT	55	55	–	55	55	55	61	66	–	–	–	59	56	56	50	–	55
Rectum	18	3D-CRT	16	16	16	16	16	16	21	21	17	18	41	19	18	19	19	16	16
		IMRT	65	65	65	65	65	66	71	71	67	68	91	69	67	68	68	66	66
	15	3D-CRT	20	20	21	21	21	21	26	26	22	23	46	24	22	23	23	21	21
		VMAT	27	27	27	27	27	27	32	33	28	29	52	31	29	30	30	28	27
Cervix	18	3D-CRT	17	17	17	17	17	18	23	24	19	20	–	21	19	20	–	18	18
		IMRT	81	81	81	81	81	82	87	88	83	84	–	85	83	84	–	82	82
	15	3D-CRT	19	19	19	19	19	19	24	25	20	21	–	22	20	21	–	19	19
		VMAT	43	43	43	43	43	43	48	45	44	45	–	46	44	45	–	43	43

Rem. = Remainder.

Table 3 – Neutron equivalent dose to organs obtained for the different tumour sites and techniques.

Location	Energy	Technique	H_T (mSv)																
			Thyroid	Lung	Breast	Stomach	Oesophagus	Liver	Colon	Urinary Bladder	Ovary	Uterus	Prostate	Red Marrow	Bone	Skin	Rem. ICRP male	Rem. ICRP female	Rem. BEIR
Prostate	18	3D-CRT	31	120	–	48	56	53	18	68	–	–	–	116	61	240	41	–	41
		IMRT	98	378	–	150	176	166	56	214	–	–	–	366	191	757	129	–	129
	15	3D-CRT	15	56	–	22	26	25	8	32	–	–	–	54	28	113	19	–	19
		VMAT	28	110	–	44	51	48	16	62	–	–	–	106	56	220	37	–	37
Rectum	18	3D-CRT	18	70	71	28	33	31	10	40	11	11	140	68	35	140	24	24	24
		IMRT	24	93	94	37	43	41	14	53	14	14	186	90	47	186	32	32	32
	15	3D-CRT	8	31	31	12	14	14	5	18	5	5	62	30	16	62	11	11	11
		VMAT	34	131	132	52	61	58	20	74	20	20	262	127	66	262	45	45	45
Cervix	18	3D-CRT	15	59	60	24	28	26	9	34	9	9	–	58	30	119	0	20	20
		IMRT	73	281	283	111	130	123	42	159	42	42	–	271	142	561	0	95	95
	15	3D-CRT	10	37	37	15	17	16	6	21	6	6	–	36	19	74	0	13	13
		VMAT	22	85	86	34	40	37	13	48	13	13	–	82	43	171	0	29	29

Rem. = Remainder.

play a countering role (i.e., one increases and the other one decreases), and for those, the change in neutron doses might not be easily predicted. For example, for the 3D-CRT rectum treatment, there are two plans one at 15 MV and the other at 18 MV (the former with a larger number of MUs). Unless the specific neutron production of each machine is characterized, R parameter in Eq. (1), it is not possible to envisage which plan is associated to the lowest/highest neutron doses. In this case the highest energy has an almost two-fold increase in second cancer risk.[1] This result was not necessarily obvious before performing the dose estimations.

However, it is complex to make a comparative assessment among techniques delivered with different machines to different tumour locations in terms of peripheral doses to a set of organs, which in turn exhibit different radiosensitivity. In order to simplify the comparison, peripheral doses were "translated" into the risk of acquiring a second primary cancer.

Maximum absorbed photon doses were in general below the limit established for the use of the simplest LNT models (Eq. (3)). Thus for SPCR estimations, this method will be used as cell sterilization effects would not present yet.

SPCR values in Fig. 2 were estimated using age-averaged risk coefficients. Although age-average is recommended in the field of radiological protection,[21] this might not be suitable for the purpose of estimating cancer risk in "identified individuals" (note that this is not the proper term as our risk estimations have been carried out with population risk factors).

Fig. 2 shows the impact, that the use of MU-demanding techniques compared to 3D-CRT at high energies, would have on *SPCR*. Nonetheless, the conclusions of the analysis should be drawn in terms not of techniques but of number of MUs as, for example, a highly wedged 3D-CRT plan can require a number of MUs which are comparable to a forward planned IMRT and, therefore, both risks would also be comparable.

Some general facts can be extracted from Fig. 2:

- ICRP recommendations lead to higher SPCR values. This is mainly due to the contribution of the risk of skin (and to a lesser extend bone) cancer, for which ICRP considers a very high incidence rate (skin's risk coefficient is approximately one order of magnitude larger than the others risk coefficients). When skin is excluded, ICRP estimations are for some cases even lower than the BEIR ones.
- When comparing cancer risks for the same treatment (e.g., rectum in this exercise), females present higher risk than males (see Fig. 2b). This is not only due to the inclusion of more organs but to a general higher radiosensitivity.
- For all pathologies the highest risk was obtained for the 18 MV IMRT planning as these plans exhibited the highest number of MUs and the highest energy. This maximum risk, if ICRP report is used, was approximately 10.3%, 4.1%, and 9.4% for prostate, rectum in a female patient, and cervix,

[1] These two treatments were delivered with different linacs for which neutron contamination was not the same and, consequently, the same number of MUs in both facilities could lead to different values of R in Eq. (1).

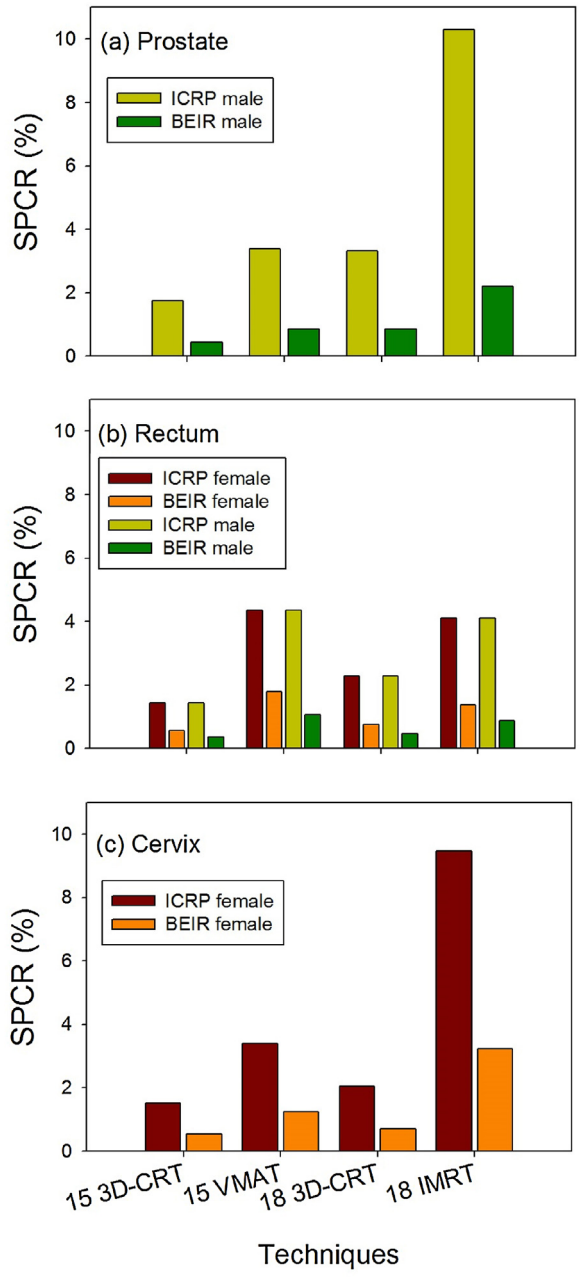

Fig. 2 – SPCR values associated with the delivered plans according to both BEIR and ICRP recommendations for (a) prostate, (b) rectum, and (c) cervix treatments.

respectively. For all pathologies, this risk decreases 5.6% on average when BEIR is used.

- The lowest risks were obtained for the 15 MV 3D-CRT planning with a very small dispersion among treatment sites (average value of 1.5% and 0.5% for ICRP and BEIR, respectively).
- Average SCPR values for the prostate case were 1.0% and 4.6% for our BEIR and ICRP estimations (bladder second cancers were excluded), respectively. Those numbers are in agreement with the 7% estimation by Berrington et al.[16] for second cancers outside the 5% isodose (i.e., excluding rectum and bladder second cancers).
- Conformal plans at both energies exhibited similar SPCR values.

For the tested scenarios, it was found that in general risks associated to VMAT plans doubled with respect to 3D-CRT plans. IMRT treatments led to an average 3-fold increase. Thus, the lower increase of risk for VMAT treatments could favour this type of planning in the face of an inverse planned IMRT. That is, when using high energy, any of the modulated techniques implied at least a 20% increase in the risk of developing a second primary cancer (following BEIR recommendations, if ICRP would have been used, they would have been at least of 30%) with respect to a conformal technique. These figures could justify the suspicion on the use of high-energy photons (e.g., >10 MV) modulated techniques though the tailoring of the high-dose volumes to the target volume could be compromised. Note that neutron contamination is different for each vendor and for Varian machines this has been estimated to be double compared with other linacs.[8–10] As a consequence, the risk values corresponding to the studied cases could have been lower if the treatments would have been delivered with linacs from other vendors.

The results of this study suggest that, mainly the intensity modulated 18 MV plans, unless forward planning or any other less MU-demanding technique is used, might not be the best way to treat pelvic cancers. For 15 MV energies, differences between VMAT and 3D-CRT were not so important, particularly for the prostate case in which the use of wedges increased the number of MU in the 3D-CRT.

It was not the aim of this exercise to find out whether low or high energy IMRT-VMAT plans were the best in terms of minimizing peripheral dose, but, to what extent, high energy IMRT-VMAT plans are a sensible alternative to high energy 3DRT in terms of peripheral doses. However, it is of interest to mention that 6 MV plans for the same three tumour locations were created and the number of MU required were. As expected, approximately 10% more than for the 15 MV plans. These larger numbers of MU did not lead to an increase in photon doses high enough to compensate for the absence of neutrons. Therefore, in all cases, the total equivalent dose at organs for 6 MV was less than for any of the 15 MV plans. However, epidemiological studies such as the one by Berrington et al.[16] on the risk of second cancers in prostate cancer survivors after RT treatments, did not find evidence that higher energy would be associated with increased second cancer risk.

4. Conclusion

This study illustrates the impact, in terms of photon and neutron equivalent dose to organs unenclosed by the 5% isodose curve, of the use of high-energy modulated techniques (IMRT and VMAT) vs. conventional ones such as 3D-CRT. Total equivalent doses were estimated be less than 1 Gy for any of the organs outside the 5% isodose and yet, responsible for average second cancers in up to 3.7% (ICRP) of patients treated with RT. It was found for the dose region studied that, in

average, peripheral doses associated to the modulated plans are around 3 times higher than for the conventional 3D-CRT. This comparative assessment was also carried out by means of two different non-threshold linear models (ICRP and BEIR), in order to assess the risk associated to these doses, with average risks of around 3.7% for ICRP and 1.1% for BEIR models.

Conflict of interest

None declared.

Financial disclosure

None declared.

Acknowledgements

Beatriz Sánchez-Nieto is in debt to Conicyt (Fondecyt N°1181133) and to the Pontificia Universidad Católica de Chile that partially funded this research through the programs "Concurso pasantías breves de investigación 2016" and Convenio Puente 2017 (N°P1702/2017). Leticia Irazola would like to thank Banco Santander for its support through the grant program "Becas Iberoamérica, jóvenes profesores y alumnos de doctorado Santander Universidad".

REFERENCES

1. Zelefsky MJ, Fuksa Z, Happersett L, et al. Clinical experience with intensity modulated radiation therapy (IMRT) in prostate cancer. *Radiother Oncol* 2000;**5**:241–9.
2. Zhang P, Happersett L, Hunt M, Jackson A, Zelefsky M, Mageras G. Volumetric modulated arc therapy: planning and evaluation for prostate cancer cases. *Int J Rad Oncol Biol Phys* 2010;**76**:1456–62.
3. Bartowiak D, Humble N, Surh P, et al. Second cancer after radiotherapy, 1981–2007. *Radiother Oncol* 2012;**10**:122–6.
4. Diallo I, Haddy N, Adidj E, et al. Frequency distribution of second cancer locations in relation to the irradiated volume among 115 patients treated for childhood cancer. *Int J Rad Oncol Biol Phys* 2009;**74**:876–83.
5. Xu XG, Bednarz B, Paganetti H. A review of dosimetry studies on external-beam radiation treatment with respect to second cancer induction. *Phys Med Biol* 2008;**5**:R193–241.
6. Gudowska I, Ardenfors O, Toma-Dasu I, Dasu A. Radiation burden from secondary doses to patients undergoing radiation therapy with photons and light ions and radiation doses from imaging modalities. *Radiat Prot Dosim* 2014;**161**:357–62.
7. National Council on Radiation Protection and Measurements. *Neutron contamination from medical accelerators. NCRP Report 79*. Bethesda: National Council on Radiation Protection and Measurements; 1984.
8. Sánchez-Doblado F, Domingo C, Gómez F, et al. Estimation of neutron equivalent dose in organs of patients undergoing radiotherapy by the use of a novel online digital detector. *Phys Med Biol* 2012;**5**:6167–91.
9. Expósito M, Sánchez-Nieto B, Terrón JA, et al. Neutron contamination in radiotherapy: estimation of second cancers based on measurements in 1377 patients. *Radiother Oncol* 2013;**10**:234–41.
10. Romero-Expósito M, Sánchez-Nieto B, Terrón JA, et al. Commissioning the neutron production of a clinical planning tool for second cancer risk estimation. *Med Phys* 2015;**42**:276–81.
11. Irazola L, Terrón JA, Sánchez-Nieto B, Bedogni R, Sánchez-Doblado F. Neutron model upgrade for peripheral neutron dose assessment evaluated in 510 radiotherapy patients. *Phys Med* 2017. S1120-1797(17)30077-7.
12. Howell RM, Koontz-Raisig W, Johnstone PAS. The trade-off between neutron dose and skin dose for 6 MV versus 18 MV for prostate IMRT: does the 20 cm rule still apply? *Int J Radiat Oncol Biol Phys* 2006;**66**:S678.
13. Thangavelu S, Jayakumar S, Govindarajan KN, Supe SS, Nagarajan V, Nagarajan M. Influence of photon energy on the quality of prostate intensity modulated radiation therapy plans based on analysis of physical indices. *J Med Phys* 2011;**36**:29–34.
14. Murray L, Henrgy A, Hoskin P, Siebert FA, Venselaar J. Second primary cancers after radiation for prostate cancer: a systematic review of the clinical data and impact of the treatment technique. *Radiother Oncol* 2014;**110**:213–28.
15. Berrington De Gonzalez A, Wong J, Kleinerman R, Kim C, Morton L, Bekelman JE. Risk of second cancers according to radiation therapy technique and modality in prostate cancer survivors. *Int J Radiat Oncol Biol Phys* 2015;**91**:295–302.
16. Sánchez-Nieto B, El-Far R, Irazola L, et al. Analytical model for photon peripheral dose estimation in radiotherapy treatments. *Biomed Phys Eng Express* 2015;**1**, http://dx.doi.org/10.1088/2057-1976/1/4/045205.
17. Howell RM, Scarboro SB, Taddei PJ, Krishnan S, Kry SF, Newhauser WD. Methodology for determining doses to in-field, out-of-field and partially in-field organs for late effects studies in photon radiotherapy. *Phys Med Biol* 2010;**55**:7009–23.
18. Gulliford SL, Koo V, Morgan RC, et al. Dose–volume constraints to reduce rectal side effects from prostate radiotherapy: evidence from MRC RT01 trial ISRCTN 47772397. *Int J Radiat Oncol Biol Phys* 2010;**7**:747–54.
19. Harrison RM. Introduction to dosimetry and risk estimation of second cancer induction following radiotherapy. *Radiat Meas* 2013;**57**:1–8.
20. International Commission on Radiological Protection. Low-dose extrapolation of radiation-related cancer risk. ICRP Publication 99. *Ann ICRP* 2005;**35**.
21. International Commission on Radiological Protection. The 2007 recommendations of the international commission on radiological protection. ICRP Publication 103. *Ann ICRP* 2007;**3**:2–4.
22. National Research Council. *Health risks from exposure to low levels of ionizing radiation: BEIR VII – phase 2*. Washington: National Academies Press; 2006.
23. Schneider U, Zwahlen D, Ross D, Kaser-Hotz B. Estimation of radiation-induced cancer from three-dimensional dose distributions: concept of organ equivalent dose. *Int J Radiat Oncol Biol Phys* 2005;**61**:1510–5.
24. Gómez F, Iglesias A, Sánchez-Doblado F. A new active method for the measurement of slow-neutron fluence in modern radiotherapy treatment rooms. *Phys Med Biol* 2010;**55**:1025–39.
25. Irazola L, Lorenzoli M, Bedogni R, et al. A new online detector for estimation of peripheral neutron equivalent dose in organ. *Med Phys* 2014;**41**:112105.
26. Irazola L, Terrón JA, Sánchez-Nieto B, Romero-Expósito M, Sánchez-Doblado F. Peripheral neutron dose model verification for real IMRT cases. *Phys Med* 2016;**32**:303.
27. Sánchez-Nieto B, Irazola L, Romero-Expósito M, Terrón JA, Sánchez-Doblado F. Validation of a peripheral photon dose model for clinical use: a prostate IMRT irradiation of the Alderson phantom. *Radioth Oncol* 2016;**119**:S381–2.

28. Shuryak I, Hahnfeldt P, Hlatky L, Sachs RK, Brenner DJ. A new view of radiation-induced cancer: integrating short- and long-term processes. Part I: approach. *Radiat Environ Biophys* 2009;**48**:263–74.

29. Shuryak I, Hahnfeldt P, Hlatky L, Sachs RK, Brenner DJ. A new view of radiation-induced cancer: integrating short- and long-term processes. Part II: second cancer risk estimation. *Radiat Environ Biophys* 2009;**48**:275–86.